Enhanced drive-by bridge modal identification via Dual Kalman filter and singular spectrum analysis

Jiantao Li[1], Xinqun Zhu[2], Jian Guo[1,3*]

[1]College of Civil Engineering, Zhejiang University of Technology, Zhejiang, China

[2]School of Civil and Environmental Engineering, University of Technology Sydney, NSW, Australia

[3]Department of Bridge Engineering, Southwest Jiaotong University, Chengdu, China

[*]Correspondence:

Jian Guo, School of Civil Engineering, Zhejiang University of Technology, Hangzhou 310023, China.

Email: Guoj@Vip.163.com

Abstract

The drive-by bridge health monitoring is to assess the bridge condition using the acceleration responses measured on the body or axle of instrumented vehicles. The vehicle responses are greatly affected by the road surface roughness that makes the bridge dynamic information blurred. Instead of direct using vehicle responses for the bridge monitoring, the dynamic response of contact point (CP) between the vehicle and bridge is further explored to enhance the drive-by bridge modal identification. A novel three-step framework is proposed to extract the components related to the bridge vibration from vehicle responses. The first step is to identify the input forces of two successive vehicles by solving the combined state-input estimation problem using Dual Kalman filter. The CP responses of two contact points are calculated using the input forces and vehicle parameters. In the second step, the subtraction technique is applied to the identified CP responses of the two instrumented vehicles and the effect of the road surface roughness can be significantly reduced. Finally, an automatic singular spectrum analysis technique (Auto SSA) is incorporated to decompose the response residual. Then the mono-component modes related to the bridge response are extracted from the response residual for drive-by bridge modal identification and/or the nonstationary characteristic identification of vehicle-bridge interaction (VBI) system. Results of numerical and experimental study demonstrate that the method can significantly suppress the vehicle response component and reduce the effect of road surface roughness to enhance the bridge modal identification.

Keywords: Vehicle-bridge interaction, roughness, contact-point response, dual Kalman filter, Auto SSA

1. Introduction

Drive-by bridge health monitoring using responses of passing vehicles has been studied for over two decades[1-3]. Unlike the traditional direct methods that require sensor instrumentation on the structure, the drive-by bridge inspection uses

instrumented vehicles to acquire and process vibration data of bridges. It facilitates a rapid and cost-effective bridge structural health monitoring approach. When a vehicle moves over the bridge, there is a dynamic coupling effect between the vehicle and bridge structure via the contact point. The vehicle is regarded as an actuator to excite the bridge vibration and also a moving sensor with proper sensor installation to capture structural dynamic responses[4]. The dynamic responses acquired from the vehicle contain the information of bridge dynamic properties which can be extracted for bridge condition assessment. The acceleration responses of passing vehicles are widely used to extract the bridge modal parameters. Yang et al.[1] proposed the method to extract bridge frequencies from the dynamic response of a passing vehicle that laid the theoretical basis of drive-by bridge modal identification. The vehicle is modelled as a sprung mass system, and the bridge is modelled as a simply supported beam considering only its first vibration mode. Damping effect of the vehicle and the bridge was ignored in the analytical formulation. Besides the modal frequencies[5], the responses of the passing vehicle were also used to estimate the damping ratio and mode shapes of bridges[6-9].

The vehicle response is a multi-component signal mainly including the components related to vehicle vibration, bridge vibration and driving motion. In VBI system, the road surface roughness has been found to have great effects on the dynamic responses of moving vehicles[10]. When moving over a rough surface, the vehicle response is amplified significantly that leads to the dominance of the vehicle frequency in its response spectrum. The bridge related dynamic information becomes less visible and further signal processing is required to enhance the bridge modal identification. Empirical model decomposition (EMD)[11] and ensemble EMD[12] were used to extract the bridge-related intrinsic mode functions. Despite the improvement of the drive-by bridge modal identification, the EMD based methods suffered from the issue of inability to extract closely spaced frequencies[13]. Singular spectrum analysis (SSA) is a data-adaptive and non-parametric method for time series decomposition and identification[14-15]. It can extract dynamic information of an underling dynamical system from noisy sampled observations. The authors[16] proposed a drive-by blind modal identification method (SSA-BSS) by combining singular spectrum analysis[17] and second-order blind identification[18]. The effectiveness of the method for the decomposition of vehicle response into different meaningful components were verified. However, the dynamic component related to the vehicle was still dominant due to the road surface roughness and the bridge related dynamic information cannot be clearly separated when there is Class B road surface roughness.

The subtraction technique using the responses of successive moving vehicles has been used to reduce the effect of road surface roughness. Yang et al.[19] proposed to use the subtraction of the response spectra of two identical successive vehicles to mitigate

the impact of road surface roughness which was found effective to enhance the drive-by identification. Malekjafarian and O'Brien[20] also found that the subtraction of the acceleration responses of two identical vehicles was helpful in reducing the effects of road surface roughness. However, these methods cannot separate the response components of the bridge from that of the vehicle. Besides, the current subtraction technique to reduce the effect of road surface roughness normally requires using identical vehicles. Despite the wide study of drive-by bridge modal identification numerically and experimentally, the effect of road surface roughness remains a significant challenge for the drive-by bridge modal identification.

Recently, it is found that the CP responses are directly related to the bridge dynamic response and are more promising for bridge modal identification than that from vehicle responses. The CP response is the response at the contact point of vehicle tire with the bridge surface which is related to the interaction force at the contact point. O'Brien et al.[21] proposed a drive-by bridge inspection via moving force identification. Higher frequency components of the forces were not well predicted due to the smoothing of the solution by regularization. Zhu et al.[22] showed that the interaction force of the VBI was more sensitive than the acceleration responses of vehicle to the bridge damage. The sensitivity of a damage indicator based on the CP responses also demonstrated it [23]. Yang et al.[24] proposed a method to use the contact-point response for the identification of bridge modal frequencies and mode shapes. The acceleration response of an undamped linear single degree of freedom (DOF) system was used to calculate the contact-point acceleration response. The driving dynamic component of the contact-point response was extracted for the bridge damage detection. However, for a multi-DOFs vehicle model, the measurement of the contact-point response is not straightforward. Nayek and Narasimhan[25] proposed an input estimation approach for the extraction of contact-point response based on a Gaussian process latent force model. The contact-point acceleration response was approximately represented with ordinary time-derivative of CP displacement as base-excited input to the vehicle. The identified contact-point response enhanced the bridge modal frequency identification, but the method can only deal with the single contact-point problems. Based on a joint input-state estimation procedure, Li et al.[26] proposed a method using the dual Kalman Filter (DKF) for the interaction force identification. The interaction forces between the two-axle vehicle and bridge were identified using acceleration responses of vehicle axles. The results showed the high accuracy of DKF for the interaction force identification which can be used for the identification of CP responses.

This study proposed a novel three-step signal process framework to extract the mono-components of the bridge from vehicle responses. In the first step, the input forces of VBI to the vehicle systems are identified using a Newmark-β based DKF model from the dynamic responses of successive vehicles and then two sets of CP

responses are obtained; In the second step, the identified CP responses are used to get response residual by subtraction; Finally, an automatic SSA[27] is incorporated to extract the mono-component of bridge response for the bridge modal identification. The study is organized as follows. Firstly, preliminaries related to the VBI model, DKF based force identification and the automatic SSA are introduced along with the proposed three-step signal process method for indirect bridge model identification. Secondly, extensive numerical studies are conducted to investigate the effectiveness of the proposed method. The pros and cons of the method comparing to the existing methods are discussed. Finally, experimental study is conducted to further demonstrate the effectiveness of the proposed method followed by the conclusions.

2. Preliminaries for the proposed method

2.1 Vehicle-bridge interaction

2.1.1 Analytical study

For a vehicle modelled as a lumped mass m_v supported on a spring of stiffness k_v moving across a simply supported beam bridge of length l with a smooth pavement and damping effect neglected, the equation of motion for the vehicle is

$$m_v\ddot{q}_v + k_v(q_v - u_c) = 0 \tag{1}$$

where q_v is the vertical displacement of the vehicle measured from the static equilibrium position; u_c is the contact-point displacement of the vehicle on the beam. The analytical solution of the vehicle and CP responses considering the first bridge vibration mode can be represented as follows[1,24]:

$$q_v(t) = \frac{\Delta_{st}}{2(1-S^2)}\left[(1-\cos\omega_v t) - \frac{\cos\left(\frac{2\pi v t}{l}\right)-\cos(\omega_v t)}{1-(2\mu S)^2} - S\frac{\cos\left(\omega_b-\frac{\pi v}{l}\right)t-\cos(\omega_v t)}{1-\mu^2(1-S)^2} + S\frac{\cos\left(\omega_b+\frac{\pi v}{l}\right)t-\cos(\omega_v t)}{1-\mu^2(1+S)^2}\right] \tag{2}$$

$$u_c(t) = \frac{\Delta_{st}}{2(1-S^2)}\left[1-\cos\left(\frac{2\pi v t}{l}\right) - S\cos\left(\omega_b-\frac{\pi v}{l}\right)t + S\cos\left(\omega_b+\frac{\pi v}{l}\right)t\right] \tag{3}$$

where ω_v is the vehicle frequency, ω_b is the frequency of the beam, $\Delta_{st} = -2m_v g l^3/EI\pi^4$, $\mu = \omega_b/\omega_v$, $S = \pi v/l\omega_b$, EI is the flexural rigidity of the beam and v is the moving speed of the vehicle. By comparing the vehicle response and CP response in Eqs. (2) and (3) respectively, it can be seen that the CP response consists of the driving component with frequency $2\pi v/l$ due to the vehicle's motion, and the bridge component with frequencies $\omega_b \pm \pi v/l$. While the vehicle response also contains the vehicle dynamic component with frequencies ω_v. Therefore, the dynamic component related to vehicle can be suppressed and the bridge dynamic component can be extracted more readily from contact-point response. The closed-form solutions of the CP responses are based on a simplified VBI model. To consider the practical

conditions, a numerical model of VBI is introduced in the following subsection.

2.1.2 Vehicle-bridge interaction modelling

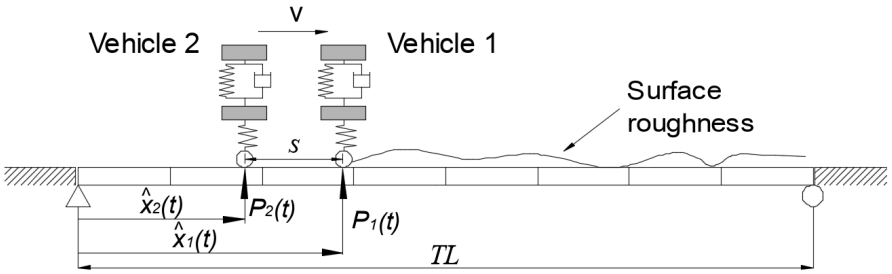

Figure 1 Simulation of the VBI model

The VBI model as shown in Figure 1 consists of the bridge model and two moving vehicles. The bridge is modelled as a simply supported beam of total span length *TL* using finite element (FE) method. The model consists of discretized beam elements with 4-DOFs each, constant mass per unit length ρ, modulus of elasticity *E*, and second moment of area *I*. The vehicle has two independent DOFs corresponding to the motion of body bounce and axle hop. Two quarter cars are instrumented with sensors to serve as sensing vehicles. The sensing vehicles first move over an approach before entering the bridge with a velocity *v* and a distance *s*. In FE model, the equation of motion of the bridge under moving vehicle loads can be expressed as:

$$\mathbf{M}_b\ddot{\mathbf{d}}_b(t) + \mathbf{C}_b\dot{\mathbf{d}}_b(t) + \mathbf{K}_b\mathbf{d}_b(t) = \mathbf{H}_c(t)\mathbf{P}_{Vint}(t) \tag{4}$$

where $\mathbf{d}_b$ denotes the vertical displacement vector of the bridge. $\mathbf{M}_b$, $\mathbf{C}_b$, $\mathbf{K}_b$ are the mass, damping and stiffness matrices of the bridge, respectively. $\mathbf{H}_c(t)$ is a function of time for the calculation of the equivalent nodal force from moving loads. The components of vector $\boldsymbol{H}_i$ $(i = 1,2)$ evaluate for the *i-th* interactive force on the *j-th* finite element.

$$\mathbf{H}_c = \begin{Bmatrix} 0 \dots 0 \dots \boldsymbol{H}_1 \dots 0 \\ 0 \dots \boldsymbol{H}_2 \dots 0 \dots 0 \end{Bmatrix}^T \in R^{NN\times 2} \tag{5}$$

$$\boldsymbol{H}_i = \begin{Bmatrix} 1 - 3\left(\frac{\hat{x}_i(t)-(j-1)l_e}{l_e}\right)^2 + 2\left(\frac{\hat{x}_i(t)-(j-1)l_e}{l_e}\right)^3 \\ (\hat{x}_i(t) - (j-1)l_e)\left(\frac{\hat{x}_i(t)-(j-1)l_e}{l_e} - 1\right)^2 \\ 3\left(\frac{\hat{x}_i(t)-(j-1)l_e}{l_e}\right)^2 - 2\left(\frac{\hat{x}_i(t)-(j-1)l_e}{l_e}\right)^3 \\ (\hat{x}_i(t) - (j-1)l_e)\left(\left(\frac{\hat{x}_i(t)-(j-1)l_e}{l_e}\right)^2 - \left(\frac{\hat{x}_i(t)-(j-1)l_e}{l_e}\right)\right) \end{Bmatrix}^T \tag{6}$$

with $(j-1)l_e \le \hat{x}_i(t) \le jl_e$ and l_e is the length of finite element. *NN* is the total

number of DOFs of the bridge structure. $\mathbf{P}_{Vint}(t) = \{P_1(t), P_2(t)\}^T = \left\{(m_{vi} + m_i)\mathrm{g} + k_t\left(y_i - r\left(\hat{x}_i(t)\right) - w(\hat{x}_i(t), t)\right), i = 1,2\right\}^T$ is the force vector at the contact points between bridge and two instrumented vehicles. y_i is the displacement response of the vehicle axle; $w(\hat{x}_i(t), t)$ is the displacement response of the bridge; and $r\left(\hat{x}_i(t)\right)$ is the height of the roughness at the contact point $\hat{x}_i(t)$.

The vehicle parameters m_v and m_1 are the masses of vehicle body and axle, respectively. k_s and c_s are the stiffness and damping of suspension spring and damper, respectively. k_t is the stiffness of the tire. The equation of motion for each vehicle can be expressed as

$$\begin{bmatrix} m_v & 0 \\ 0 & m_1 \end{bmatrix} \begin{Bmatrix} \ddot{y}_v \\ \ddot{y}_1 \end{Bmatrix} + \begin{bmatrix} c_s & -c_s \\ -c_s & c_s \end{bmatrix} \begin{Bmatrix} \dot{y}_v \\ \dot{y}_1 \end{Bmatrix} + \begin{bmatrix} k_s & -k_s \\ -k_s & k_s + k_t \end{bmatrix} \begin{Bmatrix} y_v \\ y_1 \end{Bmatrix} = \begin{Bmatrix} 0 \\ k_t d_{cp}(t) \end{Bmatrix} \quad (7)$$

where y_v and y_1 are the displacement responses of the vehicle body and axle, respectively. $d_{cp}(t) = w(\hat{x}_i(t), t) + r\left(\hat{x}_i(t)\right)$ is the displacement of contact point with location at $\hat{x}_i(t)$. Eq. (7) can be rewritten as

$$\mathbf{M}_v\ddot{\mathbf{d}}_v(t) + \mathbf{C}_v\dot{\mathbf{d}}_v(t) + \mathbf{K}_v\mathbf{d}_v(t) = \mathbf{D}F_{cp}(t) \quad (8)$$

where $\mathbf{D} = [0,1]^T$ and $F_{cp}(t) = k_t d_{cp}(t)$.

The road surface roughness in time domain can be simulated from[28]

$$r(x) = \sum_{i=1}^{N_f} \sqrt{4S_d(f_i)\Delta f} \cos(2\pi f_i x + \theta_i) \quad (9)$$

where $S_d(f)$ is the displacement power spectral density of the road surface roughness, $f_i = i\Delta f$ is the spatial frequency(cycles/m), $\Delta f = 1/N_f\Delta$, Δ is the distance interval between successive ordinates of the surface profile, N_f is the number of data points, and θ_i is a set of independent random phase angle uniformly distributed between 0 and 2π. Class B road surface roughness from ISO (8606)[29] is used in the simulation to represent a road profile in a good condition.

2.2 CP response identification with Newmark-β based DKF

2.2.1 The state space representation of the vehicle dynamic system

In the right-hand side of Eq. (8), $F_{cp}(t)$ is the unknown input force to the vehicle system that is directly related to the CP response. The identification of the force is a joint state-input estimation problem that can be solved by using the Newmark-β based DKF[26]. After $F_{cp}(t)$ is identified, the CP response can be obtained by

$$d_{cp}(t) = F_{cp}(t)/k_t \quad (10)$$

The input force of the vehicle system is identified based on a state space representation of Eq.(8) using Newmark-β based DKF. In the following formulation, the state of

vehicle $\mathbf{d}_v(t)$ is replaced by $\mathbf{x}$ for conciseness. The state space representation of the vehicle dynamic is written as follows

$$\mathbf{X}_{k+1} = \mathbf{A}\mathbf{X}_k + \mathbf{B}F_{cp_{k+1}} \tag{11}$$

where $\mathbf{X}_k = [\mathbf{x}_k^T\ \dot{\mathbf{x}}_k^T\ \ddot{\mathbf{x}}_k^T]^T$ is a state vector; $\mathbf{x}_k$ is the state at *k-th* time step. The derivation of the state space representation based on Newmark-β and the forms of matrices $\mathbf{A}$ and $\mathbf{B}$ are presented in Appendix A.

2.2.2 Measurements

The measured acceleration, velocity and displacement responses of the vehicle are $\ddot{\mathbf{x}}_k, \dot{\mathbf{x}}_k, \mathbf{x}_k$ respectively. They can be assembled as a vector $\mathbf{y}_k \in R^{ns\times 1}$

$$\mathbf{y}_k = \mathbf{R}_a\ddot{\mathbf{x}}_k + \mathbf{R}_v\dot{\mathbf{x}}_k + \mathbf{R}_b\mathbf{x}_k \tag{12}$$

where $\mathbf{R}_a$, $\mathbf{R}_v$ and $\mathbf{R}_b \in R^{ns\times NV}$ are the output influence matrices for the measured acceleration, velocity and displacement, respectively, ns is the dimension of the measured responses and NV is the number of DOFs of the vehicle.

Letting $\mathbf{R} = [\mathbf{R}_d\ \mathbf{R}_v\ \mathbf{R}_a]$, Eq.(12) can be rewritten into the following discrete form as

$$\mathbf{y}_k = \mathbf{R}\mathbf{X}_k \tag{13}$$

2.2.3 State-space model

The state space model of the vehicle system can be obtained by combining Eqs. (11) and (13) as

$$\begin{cases} \mathbf{X}_{k+1} = \mathbf{A}\mathbf{X}_k + \mathbf{B}F_{cp_{k+1}} + \boldsymbol{v}_k^{\boldsymbol{x}} & \text{(14a)} \\ \mathbf{y}_k = \mathbf{R}\mathbf{X}_k + \boldsymbol{w}_k & \text{(14b)} \end{cases}$$

where $\boldsymbol{v}_k^{\boldsymbol{x}}$ and $\boldsymbol{w}_k$ are the process noise and the measurement noise vectors respectively representing uncertainties in the modelling and the measurement processes respectively. The noise vectors $\boldsymbol{v}_{\boldsymbol{k}}^{\boldsymbol{x}}$ and $\boldsymbol{w}_k$ are assumed Gaussian white with covariance $\boldsymbol{Q}^{\boldsymbol{x}}$ and $\boldsymbol{Q}^{\boldsymbol{y}}$ respectively. A reduced state $\overline{\mathbf{X}}_k = \mathbf{X}_k - \mathbf{B}\mathbf{P}_k$ can be further formulated by transforming Eq. (14) as

$$\begin{cases} \overline{\mathbf{X}}_{k+1} = \mathbf{A}\overline{\mathbf{X}}_k + \mathbf{A}\mathbf{B}F_{cp_k} + \boldsymbol{v}_k^{\boldsymbol{x}} & \text{(15a)} \\ \mathbf{y}_k = \mathbf{R}\overline{\mathbf{X}}_k + \mathbf{R}\mathbf{B}F_{cp_k} + \boldsymbol{w}_k & \text{(15b)} \end{cases}$$

For the joint input-state estimation, a random walk model is introduced to represent the state equation for the input F_{cp} as

$$F_{cp_{k+1}} = F_{cp_k} + v_k^p \tag{16}$$

where v_k^p is a zero mean Gaussian white process with covariance matrix Q^p. Combining Eqs. (15b) and (16) gives a new state-space equation for the input as

$$\begin{cases} F_{cp_{k+1}} = F_{cp_k} + v_k^p & (17a) \\ \mathbf{y}_k = \mathbf{R}\mathbf{B}F_{cp_k} + \mathbf{R}\bar{\mathbf{X}}_k + \boldsymbol{w}_k & (17b) \end{cases}$$

where the observation is $\mathbf{y}_k$, and the state is F_{cp_k}. A sequential implementation of the Kalman Filter described in Eqs. (15) and (17) can give the state $\mathbf{X}_k$ and input force F_{cp_k}.

2.2.4 Implementation of the DKF

The implementation of DKF is described as following:

1) Initialization of the state and input force at t_0

Estimation of the initial state $\bar{\mathbf{X}}_0$ and input force value F_{cp_0} and their corresponding covariance matrices $\mathbf{G}_0^{\boldsymbol{x}}$ and G_0^F

2) For each time instant t_k $(k = 1, \dots, N_t)$

- Prediction stage for the input

  Evolution of the input and prediction of covariance with

  $$F_{cp_k}^{-} = F_{cp_{k-1}}; \qquad \mathrm{G}_k^{F-} = \mathrm{G}_{k-1}^F + Q^p$$

- Update stage for the input

  Kalman gain for input with

  $\mathrm{K}_k^F = \mathrm{G}_k^{F-}\mathbf{J}^{\boldsymbol{T}}(\mathbf{J}\mathrm{G}_k^{F-}\mathbf{J}^{\boldsymbol{T}} + \boldsymbol{Q}^{\boldsymbol{y}})^{-1}$

  where $\mathbf{J} = \mathbf{R}\mathbf{B}$

  Improved predictions of input with

  $$F_{cp_k} = F_{cp_k}^{-} + \mathrm{K}_k^F(\mathbf{y}_k - \mathbf{J}F_{cp_k}^{-} - \mathbf{R}\bar{\mathbf{X}}_{k-1}); \qquad \mathrm{G}_k^F = \mathrm{G}_k^{F-} - \mathrm{K}_k^F\mathbf{J}\mathrm{G}_k^{F-}$$

- Prediction stage for the state:

  Evolution of state and prediction of covariance of state with

  $$\bar{\mathbf{X}}_k^{-} = \mathbf{A}\bar{\mathbf{X}}_{k-1} + \mathbf{A}\mathbf{B}F_{cp_k}; \qquad \mathbf{G}_k^{\boldsymbol{x}-} = \mathbf{A}\mathbf{G}_{k-1}^{\boldsymbol{x}}\mathbf{A} + \boldsymbol{Q}^{\boldsymbol{x}}$$

- Update stage for the state

  Kalman gain for state：

  $$\mathbf{K}_k^{\boldsymbol{x}} = \mathbf{G}_k^{\boldsymbol{x}-}\mathbf{R}^{\boldsymbol{T}}(\mathbf{R}\mathbf{G}_k^{\boldsymbol{x}-}\mathbf{R}^{\boldsymbol{T}} + \boldsymbol{Q}^{\boldsymbol{y}})^{-1}$$

  Improved predictions of state：

  $$\bar{\mathbf{X}}_k = \bar{\mathbf{X}}_k^{-} + \mathbf{K}_k^{\boldsymbol{x}}(\mathbf{y}_k - \mathbf{R}\bar{\mathbf{X}}_k^{-} - \mathbf{J}F_{cp_k}); \qquad \mathbf{G}_k^{\boldsymbol{x}} = \mathbf{G}_k^{\boldsymbol{x}-} - \mathbf{K}_k^{\boldsymbol{x}}\mathbf{R}\mathbf{G}_k^{\boldsymbol{x}-}$$

The detailed description on parameter initialization of DKF is discussed in [26,31]

2.3 Auto SSA

The identified $d_{cp}(t)$ from Eq. (10) consists of bridge response and road surface roughness at the contact point as described in Eq.(7). The road surface roughness has a significant effect on the vehicle response. When the responses of the two contact points are obtained, the response residual denoted as vector $\mathbf{d}_{rcp}$ can be calculated by subtracting the time-shifted response of the second CP from the response of the first CP. The time interval for shifting the second set of CP response is $\Delta t = s/v$. The response residual is related to the driving components and bridge dynamic components. To eliminate the effect of driving component and extract the mono-components related to the bridge response, an automatic SSA method is introduced to decompose the residual of CP responses. The SSA is briefly introduced.

2.3.1 The singular spectrum analysis method

There are two successive stages for performing the SSA, i.e. decomposition and reconstruction. In the decomposition stage, the CP response residual $\mathbf{d}_{rcp}(t)$ is mapped into a trajectory matrix with K lagged column vectors of length L. The trajectory matrix $\mathbf{Z}$ is then expanded into a sum of weighted elementary matrices using Singular Value Decomposition (SVD). In the reconstruction step, the elementary matrices are split into disjoint groups and summing the matrices within each group. The grouping procedure can be determined based on the information contained in the singular vectors and in the singular spectrum. A skew diagonal averaging procedure is implemented to the grouped matrices to recover time series referred to as elementary components. The SSA finally expands the time series into a set of components $\boldsymbol{d}^{(l)}$ $(l = 1,2, \ldots N_{\mathrm{g}})$. The flowchart of SSA is presented in Figure 2 and the detailed information of SSA can be found in [32].

2.3.2 Automatic SSA

Aiming at making the SSA automatic and adaptive for any component type, Harmouche et al.[27] proposed an Auto SSA method to extract the physically interpretable components of a time series. The agglomerative hierarchical clustering[33] was adopted to apply the automatic grouping to the elementary component. The Auto SSA is adopted to extract the components from the CP response residual.

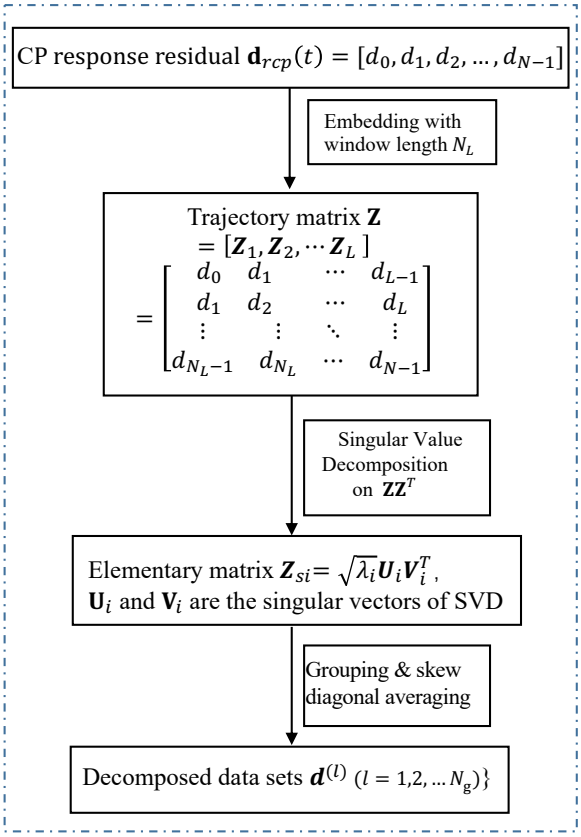

Figure 2 Flowchart of the SSA

2.4 The proposed drive-by bridge modal identification method

To reduce the effects of road surface roughness and extract the bridge dynamic components, a framework is proposed to process the vehicle acceleration responses. Two instrumented vehicles with a constant distance are used to measure the vehicle axle responses during their moving over the bridge with same speed. The measured vehicle responses are firstly input to the state space model of the vehicle to get the input forces of the vehicles at the contact points using DKF. The displacement responses at two contact points are calculated with the identified forces. After shifting the response of the second contact point to the same location of the first contact point with the time interval Δt, the response residual is obtained by subtracting the response of the first contact point to that of the second one. After this procedure, the road roughness can be significantly reduced. The response residual mainly consists of the components related to the driving frequency and bridge frequency. Finally, the Auto SSA is used to extract the bridge dynamic components. A flowchart of the proposed method for the enhancement of drive-by bridge modal analysis is given in Figure 3.

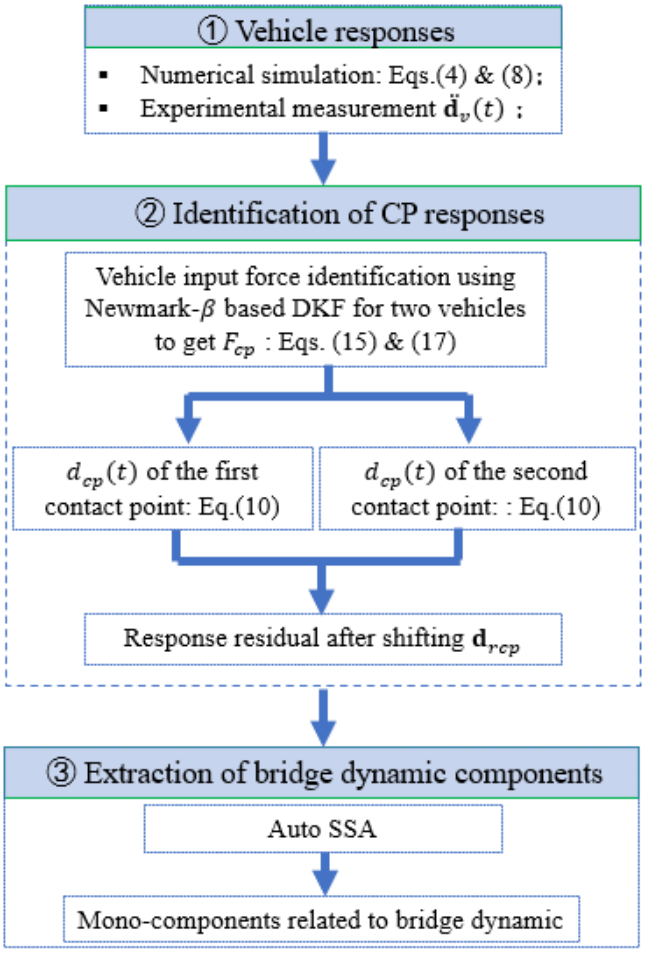

Figure 3 Flowchart of the proposed bridge modal identification method

3 Numerical study

Numerical study is conducted to analyze the effectiveness of the proposed method in enhancing the drive-by bridge modal identification and extracting the mono-components related to bridge dynamic information. The properties of the bridge are: $TL = 35\text{m}, \rho = 5000\,\text{kg/m}$, $EI = 2.178\text{e}10\ \text{Nm}^2$. The damping ratio is set as 0.01 and the first three theoretical bridge modal frequencies are 2.68, 10.71 and 24.09Hz, respectively. The bridge is divided into 20 finite elements. The properties of the vehicles are given in Table 1. The mass ratio between vehicle and bridge is 0.86% that is small enough to assume that the vehicle does not change the dynamic properties of the bridge. The distance between two vehicles is 2 m. The equations of motion of VBI system presented in Eqs.(4) and (8) are solved to simulate the vehicle acceleration responses. Moving speed of vehicles is 4m/s and sampling frequency is set as 200Hz. The fast Fourier transform (FFT) with rectangular window is used to calculate the spectrum of response. The length of response data is used as the number of data point in performing FFT.

Table 1 Properties of quarter-car model

Property	Unit	Symbol	Quarter car model
Body mass	kg	m_v	1000
Axle mass	kg	m_1	500
Suspension stiffness	N/m	k_s	2.47e5
Suspension damping	N s/m	c_s	3.00e3
Tire stiffness	N/m	k_t	5.50e5
Frequency of vehicle bounce	Hz	f_{bounce}	2.02
Frequency of axle hop	Hz	f_{axle}	6.52

3.1. Comparison of the identification using vehicle responses and CP responses

3.1.1 Vehicles moving over smooth road surface

The first case is two identical vehicles moving over a bridge with a smooth road profile. The acceleration responses of vehicle axles and the response spectrum are given in Figure 4. The response and spectrum results are normalized by dividing each data by the maximum absolute value, respectively. From the spectrum, it can be seen that the acceleration responses contain the dynamic information related to the vehicle, bridge and driving frequencies. The first bridge frequency dominates the response spectrum that can be easily identified. Figure 5 presents the contact-point displacements and response spectrum of the VBI model. No vehicle related frequency component is identified from the spectra. The numerical results are consistent with the analytical analysis that the contact-point response can suppress the vehicle dynamic component to enhance the drive-by bridge modal identification.

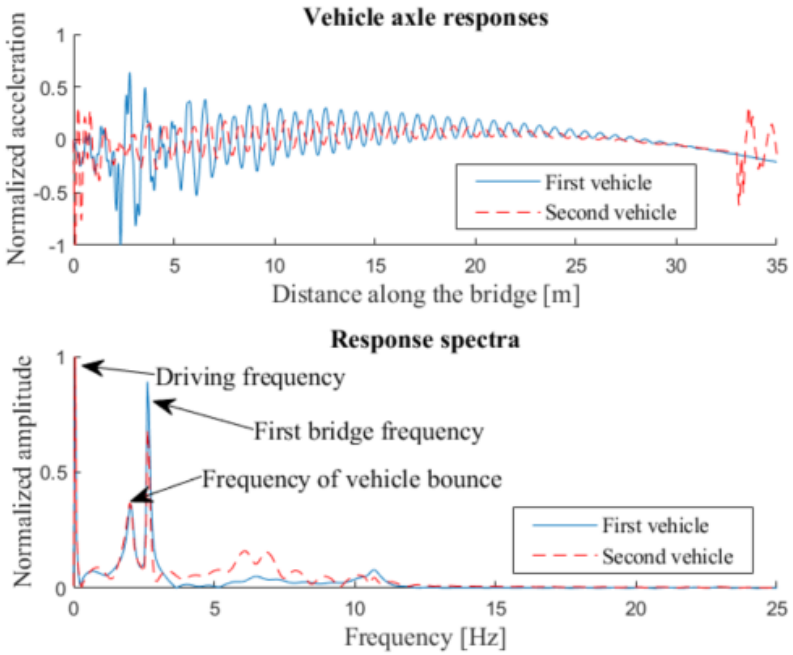

Figure 4 Vehicle axle responses and response spectra

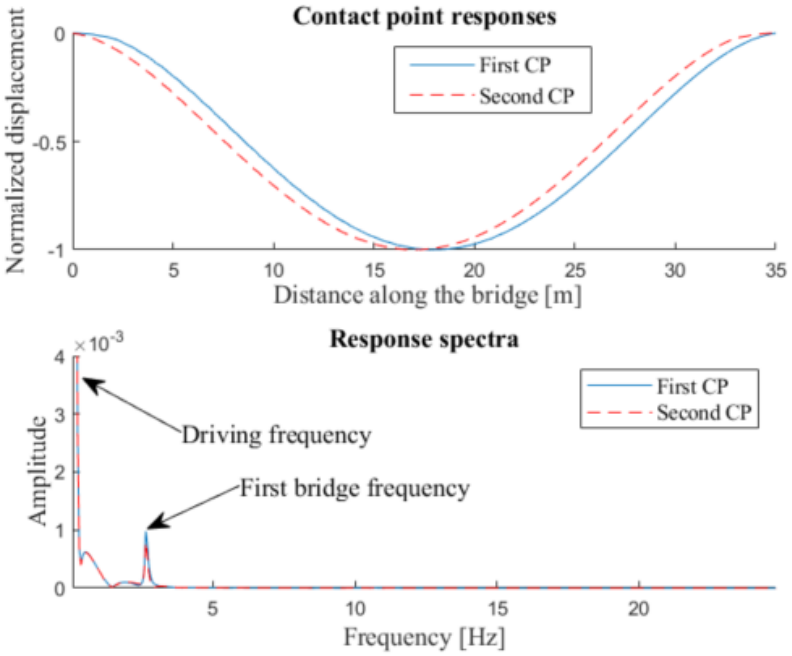

Figure 5 Contact-point responses and response spectra

3.1.2 Vehicles moving over rough road surface

Road surface roughness has great effects on the vehicle dynamic responses. When a class B rough road surface is considered, the vehicle axle acceleration and CP displacement of the first vehicle are computed. The normalized dynamic responses (divided by the maximum absolute value of the responses) and the spectra are shown in Figure 6. The spectrum of the vehicle response is dominated by the vehicle frequency and the driving component dominates the spectrum of the contact-point response. The bridge related dynamic information is hardly visible. The response residuals are therefore calculated with two sets of responses from two vehicles and contact points, respectively. The response residuals and the spectra are given in Figure 7. The first bridge frequency is observed. The results demonstrate that the subtraction technique can reduce the effect of road surface roughness and improve the visibility of the bridge dynamic information. However, the spectrum of the vehicle response residual still contains notable dynamic components related to vehicle. The amplification of the driving frequency near the vehicle frequency may cause confusions when determining the bridge modal frequencies from the spectrum of vehicle response residual.

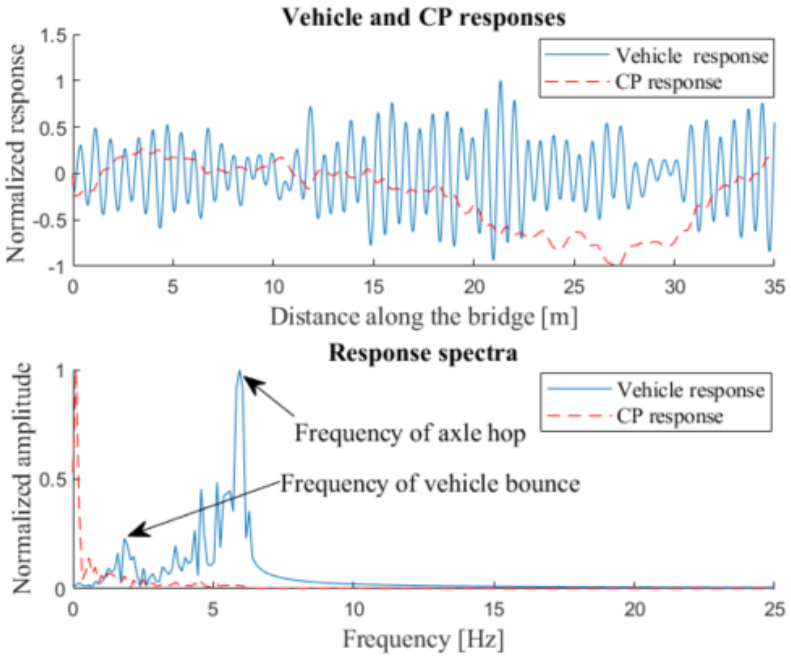

Figure 6 Normalized responses of vehicle and contact point and their spectra

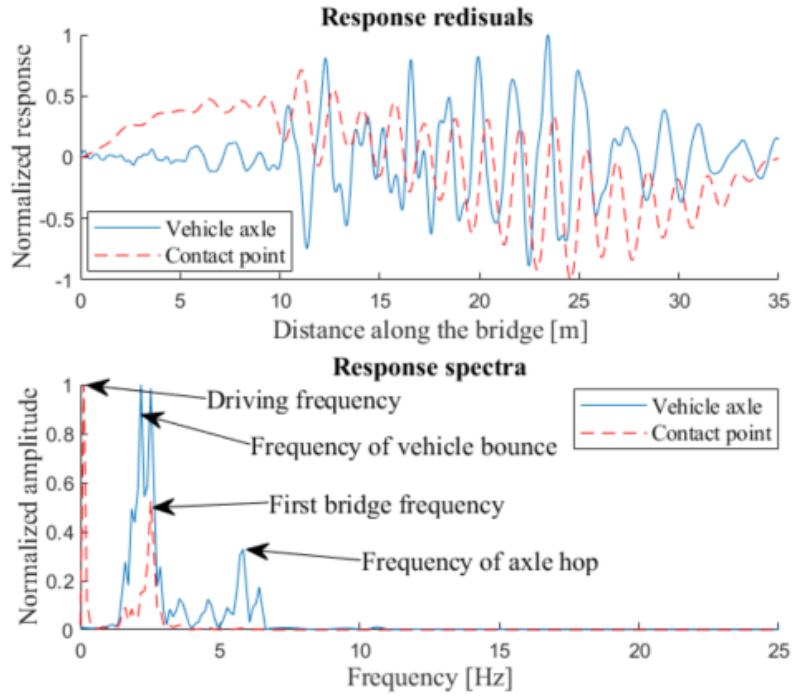

Figure 7 Response residuals of vehicle and contact point and their spectra

3.2 Identification of CP displacement responses

The numerical study above shows the effects of the road surface on the drive-by bridge modal identification. The results demonstrate the effectiveness of the subtraction technique in reducing the effect on road surface roughness and enhancing the visibility of bridge modal parameters. Compared to the vehicle responses, the contact-point responses can suppress the dynamic component related to the vehicle and make the

identification of bridge modal frequency more straightforward. In an actual situation, the contact-point responses cannot be measured directly. Therefore, the CP responses are identified from vehicle responses using the proposed method. In the following subsections, the response residual from the two sets of contact-point responses is presented to verify the accuracy of the proposed method.

The CP responses at two contact points are identified using the DKF, and the response residuals are calculated for smooth and rough bridge road surface, respectively. Figure 8 shows the response residuals and the spectra for different bridge surface conditions. It can be seen that the identified responses using DKF match very well with the true values. Besides, for the rough road surface condition, an enhancement of the bridge response components is observed from the response spectrum. The reason is that the road surface roughness amplifies the vehicle responses and the bridge dynamic response.

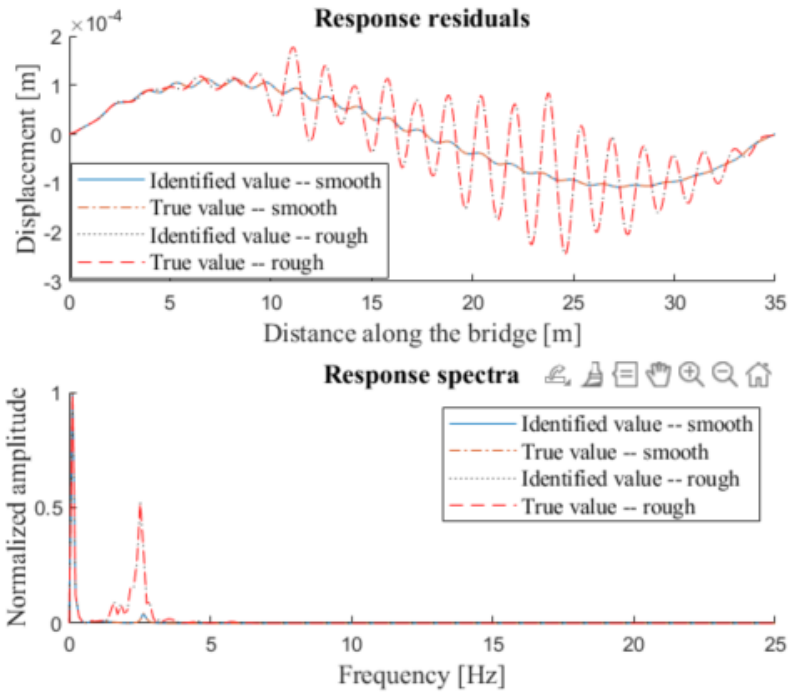

Figure 8 Response residuals of contact points and their spectra

3.3 Parametric study

3.3.1 Effect of vehicle parameters

In the previous study, two identical vehicles are used for the measurement. Actually, the proposed method can identify bridge frequencies using two different vehicles or a two-axle vehicle. Therefore, the parameters of the first vehicle remain the same as in previous subsection and those for the second vehicle are given in Table 2 which are adopted from [34]. The response residuals of the vehicle responses and the identified CP responses are presented in Figure 9 along with the response spectra. From

the spectra of the response residuals, it can be seen that when two sensing vehicles with different parameters are used, the subtraction technique is more effective to reduce the effect of roughness for the CP responses than for vehicle responses. Therefore, the proposed method can be applied to vehicles with different parameters, such as using a two-axle vehicle model.

Table 2 Properties of the second quarter-car model

Property	Unit	Symbol	Quarter car model
Body mass	kg	m_v	1600
Axle mass	kg	m_1	160
Suspension stiffness	N/m	k_s	1.00e5
Suspension damping	N s/m	c_s	5.00e3
Tire stiffness	N/m	k_t	3.00e5
Frequency of vehicle bounce	Hz	f_{bounce}	1.09
Frequency of axle hop	Hz	f_{axle}	7.98

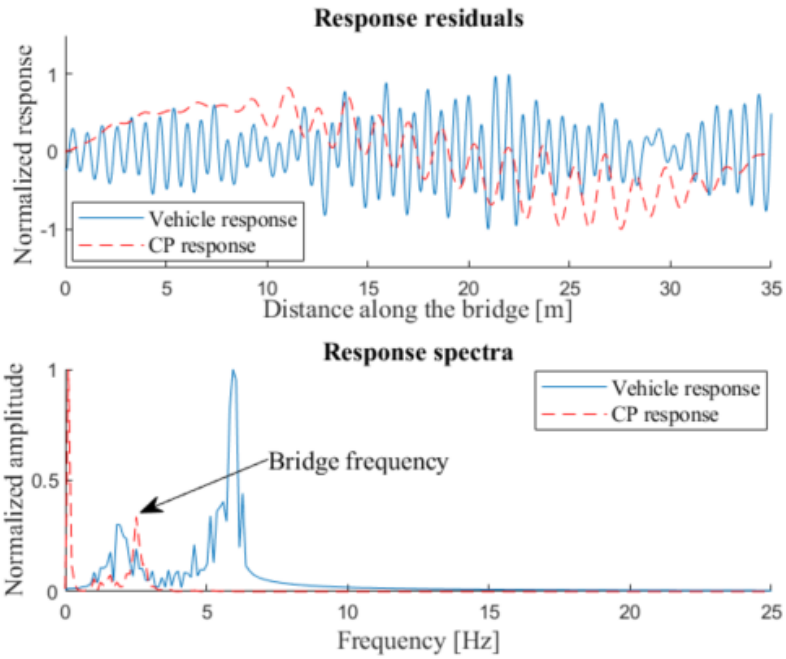

Figure 9 Response residuals and their spectra using different vehicles

3.3.2 Effect of operational load

During the drive-by inspection of the bridge, there may be other operational force, such as traffic. Therefore, the operational load is considered as a random moving force in the VBI model[35]. When the moving operational load $P_{ran}(t)$ is incorporated into the VBI system, the motion of equation of bridge Eq. (4) becomes

$$\mathbf{M}_b\ddot{\mathbf{d}}_b(t) + \mathbf{C}_b\dot{\mathbf{d}}_b(t) + \mathbf{K}_b\mathbf{d}_b(t) = \mathbf{H}_c(t)\mathbf{P}_{Vint}(t) + \mathbf{H}_r(t)P_{ran}(t) \quad (18)$$

where $\mathbf{H}_r(t)$ is the function for the calculation of the equivalent nodal force from

moving load $P_{ran}(t)$. The operational load moves over the bridge before the entrance of the inspection vehicles with the moving speed $v_p = TL/(TL + L_{ap})\, v$, where TL is the length of bridge, L_{ap} is the length of approach and v is the speed of vehicle. The time series of the simulated operational load is shown in Figure 10. The CP response residual when two identical inspection vehicles are used is shown in Figure 12. It is found that the first bridge modal frequency becomes more obvious when the operational load is considered. The presence of the operational load amplifies the bridge dynamic and is beneficial for the modal identification from the contact-point responses.

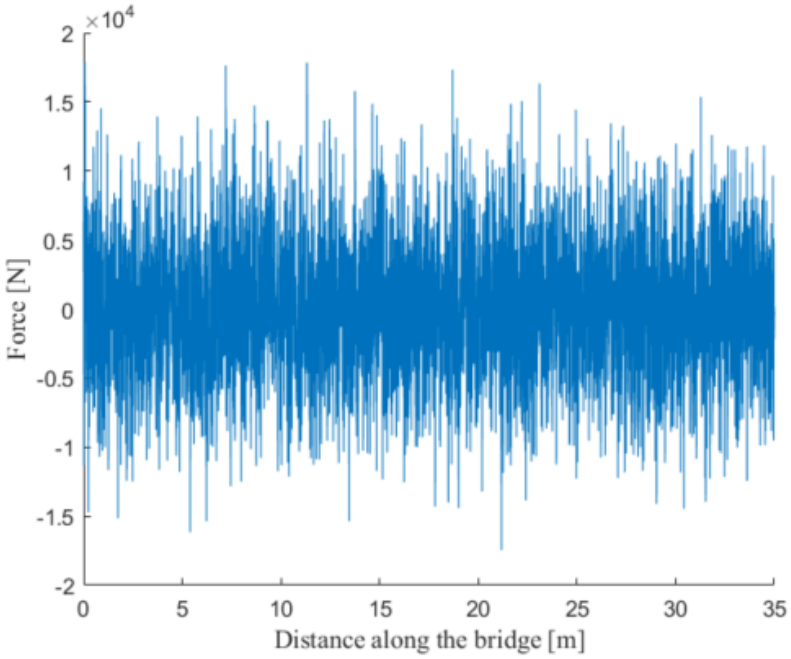

Figure 10 Moving operational load

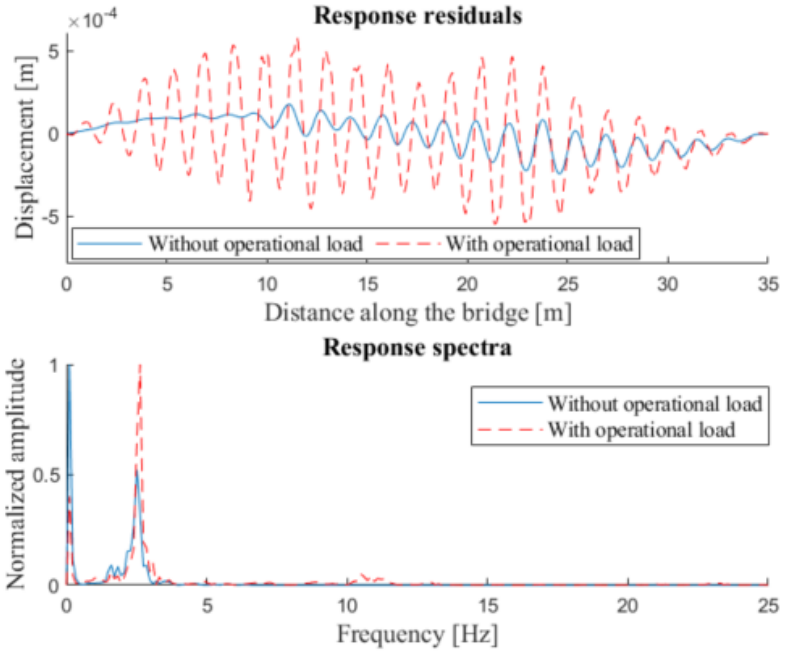

Figure 11 Response residuals of CP and their spectra

3.3.3 Effect of moving speed

The effect of moving speed on identification of the contact-point response is studied. The identified response residual when moving speed is 8 m/s is presented and compared to that when moving speed is 4 m/s, as shown in Figure 12. It can be seen that the contact-point responses are identified with high accuracy for different vehicle moving speeds. However, a lower moving speed can identify the bridge modal frequency with higher precision.

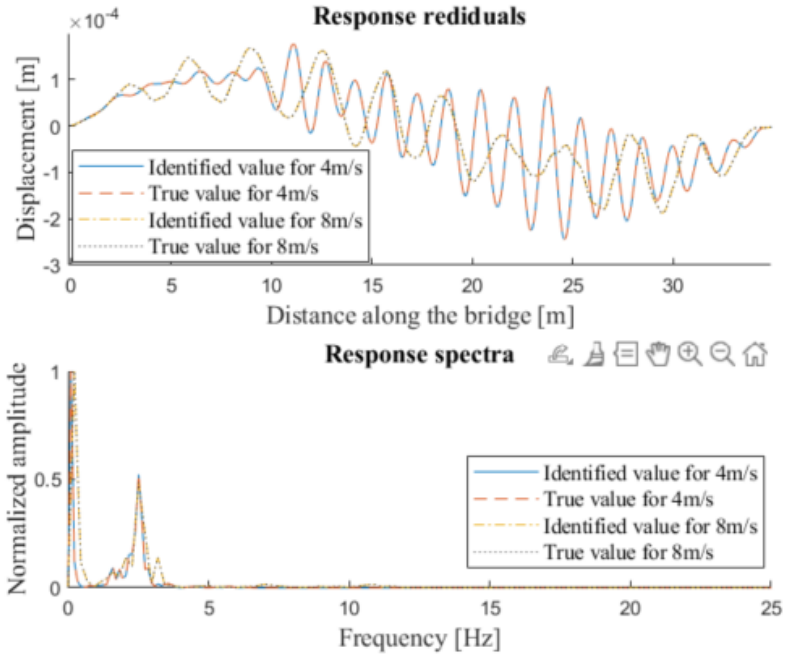

Figure 12 Response residuals of CP and their spectra for different speeds

To mitigate the unwanted road roughness effects, the speed of the front and rear vehicle axles should keep constant during the measurement. To investigate the effects of the error of the vehicle speed measurement on the identification, an adjustment term is introduced to calculate the time interval Δt for the time shifting in the substruction procedure. Considering the general case, the error of the measured speed is 5%. The time interval will be $\Delta t = s/(1 \pm 5\%)v$. Figure 13 shows the response residuals and their spectra with and without considering the operational load to the bridge. When no operational load of bridge is considered, it can be seen that the variation of the moving speed makes it difficult to eliminate the effects of road roughness. The bridge related dynamic component is not visible. However, when the operational load as shown in Figure 10 is considered, it can be seen that the bridge related dynamic components can be identified from the spectrum of CP response residual. Therefore, the speed of vehicles axles should be monitored accurately to eliminate the road surface roughness effectively. It is beneficial to conduct the drive-by modal identification when the bridge is subjected to a large operational load.

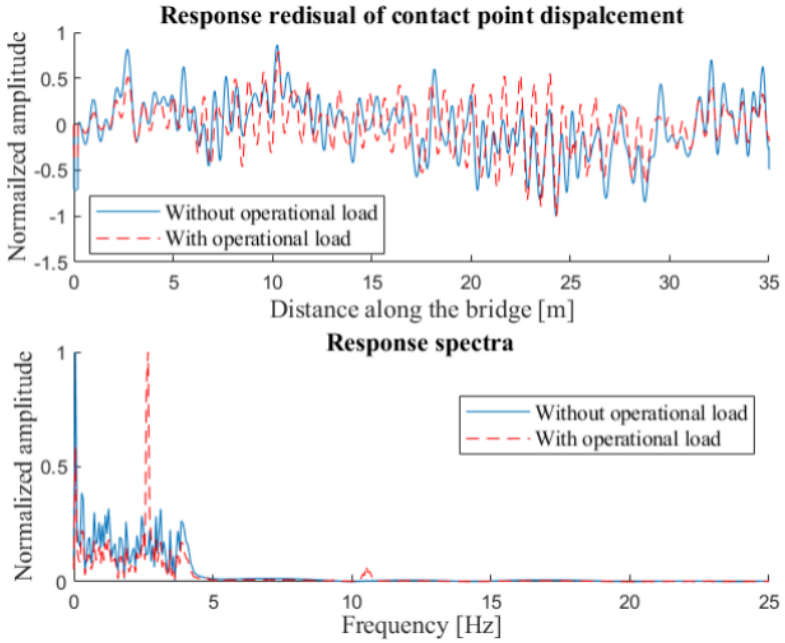

Figure 13 Response residuals of CP and their spectra for a varying vehicle speed

3.3.4 Effect of measurement noise

The identified CP responses for the noise-free condition using the proposed method is very accurate compared to the true value. However, the actual measured vehicle responses contain measurement noise. To assess the performance of the proposed approach with noise contaminated signals, two scenarios with 5% and 10% noise are considered. The noisy measurement is simulated as[25]:

$$y_{\text{noisy}} = y_{\text{true}} + \frac{\text{noise\%}}{100} \times \text{SD}(y_{\text{true}}) \times \text{WGN} \tag{19}$$

where, y_{true} is the true vehicle acceleration response, $\text{noise\%}$ is the noise level in percentage, $\text{SD}(y_{\text{true}})$ is the standard deviation of y_{true} and WGN is the Gaussian white noise. The response residuals of the contact points considering Class B road surface roughness and different noise levels are presented in Figure 14. It can be seen that the measurement noise has significant effects on the identified CP responses. The identified values are found deviate from the true values. Despite of the deviation of the response residual in time domain, the spectra of the responses are less sensitive to the measurement noise.

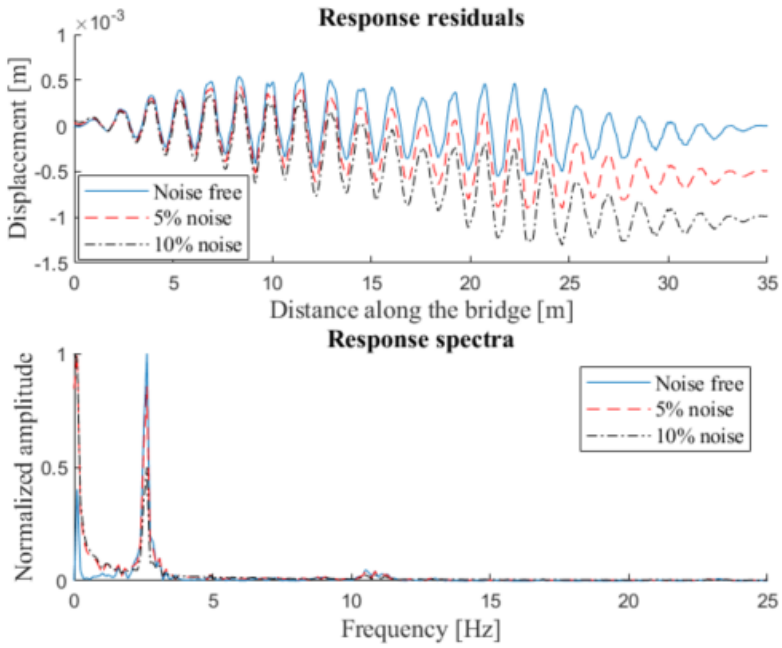

Figure 14 Response residuals of CP and their spectra for different measurement noise

3.3.5 Extraction of the mono components from noisy measurement by Auto SSA

From the previous numerical study, it can be seen that the spectrum of the response residual of contact point is usually dominated by the driving frequency. Therefore, the Auto SSA is applied to the response residual to extract the mono components related to the bridge dynamic information. The Auto SSA is applied to the response residual identified by DKF to extract the response components considering different measurement noise. The identified components and the spectra are shown in Figure 15. Three components are extracted from the response residuals with the component 1 corresponding to the driving frequency and the other two corresponding to the bridge modal frequencies. It can be seen that the Auto SSA can extract the mono-components related to bridge accurately and enhance the drive-by modal identification. The extracted bridge-related components also show robustness to the measurement noise using the proposed method. EMD is also used to extract bridge dynamic components from the identified response residual for comparison. The extracted bridge dynamic components using two methods are shown in Figure 16. It can be seen that the Auto SSA outperforms the EMD in separating the mono-components related to the bridge dynamic response.

A SSA based method SSA-BSS in previous study[16], is used to analyze the response residual of vehicle axles to identify the bridge dynamic components for comparison with current method. Three components are extracted and the normalized components and spectra are presented in Figure 17. Mode 1 and Mode 3 are related to the vehicle frequencies and Mode 2 is related to the first bridge frequency. Compared to the results in Figure 15, it can be seen that the component related to the first bridge

frequency using previous method contains some part of the component related to vehicle dynamics. Besides, the previous method fails to identify the second bridge frequency. The results demonstrate that the proposed method is more capable of reducing the effects of vehicle dynamic information due to road surface roughness and extracting clear mode related to bridge dynamics. Moreover, the Auto SSA used in this study can perform decomposition more effectively compared to the previous SSA based method.

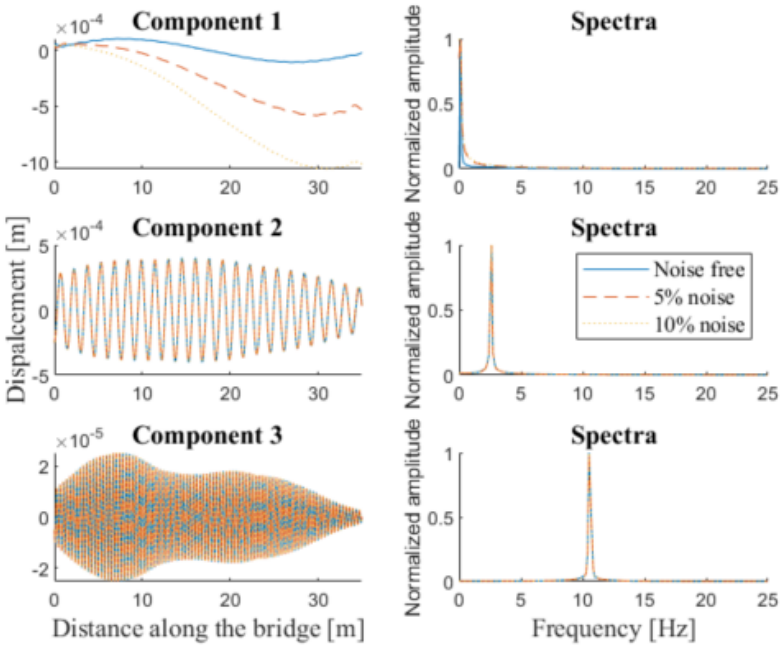

Figure 15 Components extracted from response residual with auto SSA

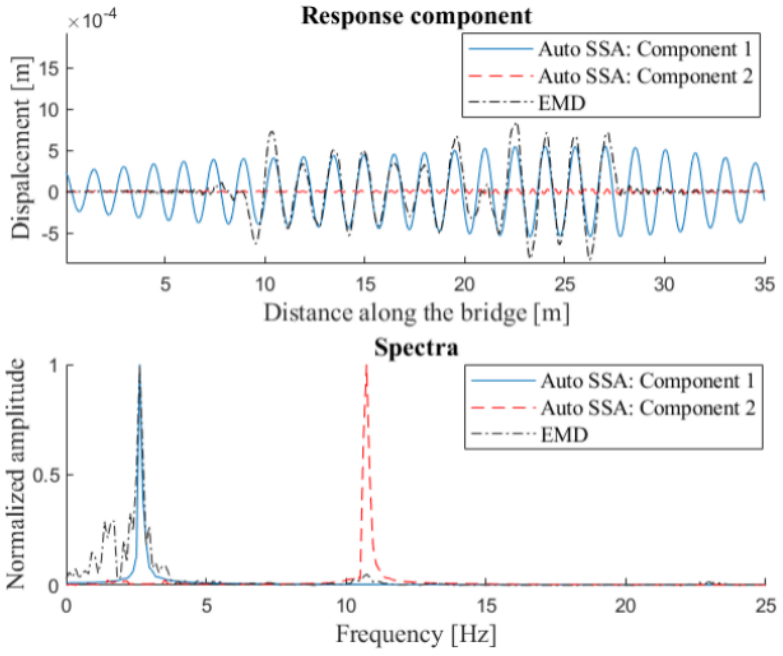

Figure 16 Using Auto SSA and EMD to extract bridge dynamic components

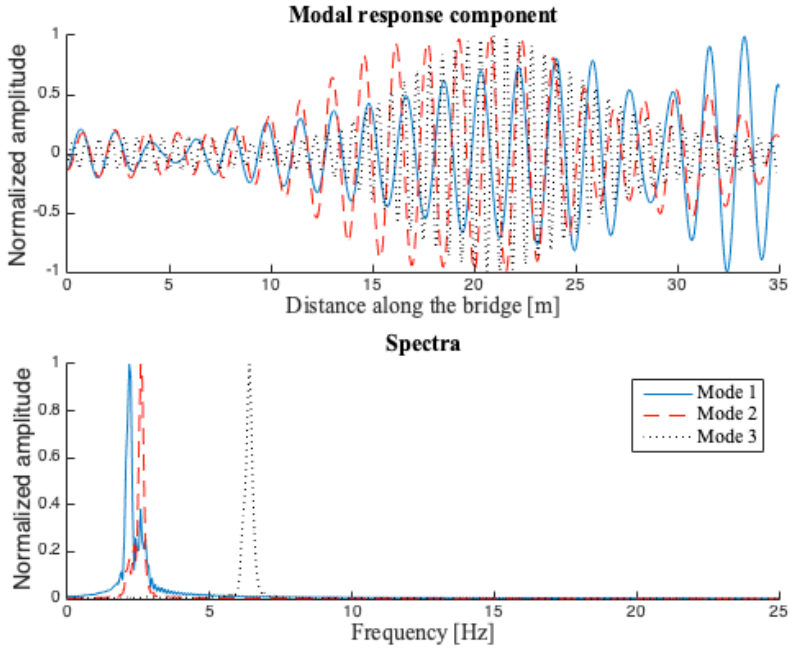

Figure 17 Bridge dynamic component extraction using SSA-BSS

3.4 The nonstationary characteristics of the VBI system

The numerical study in Section 3.1 to Section 3.3 applies light measuring vehicles for the bridge modal identification. The mass ratio between the vehicle and bridge is less than 1%. Therefore, it is assumed that the vehicle properties do not change the bridge dynamic properties and only the constant bridge modal frequencies are identified. In the VBI system, the locations of the inspection vehicles are time-varying due to the moving nature. Therefore, the dynamic response of the VBI system is nonstationary, especially when heavy vehicles are used as the moving sensor and actuator at the same time. The inherent nonstationary characteristics can reveal important information of the actual dynamic interaction. A commonly used two-axle car model is used in the VBI system as shown in Figure 18. There are four independent DOFs corresponding to sprung mass bounce displacement, y_v, pitch rotation, θ_v, and axle hop displacement of the unsprung masses at front and rear axles, y_1 and y_2, respectively. For the generality, two vehicle models of different properties are adopted for the VBI analysis. The parameters of vehicle Model 1 are gathered from the literature[21,36] and that of vehicle Model 2 are from the literature[37] neglecting the damping of the vehicle tires. The parameters of the vehicle models are listed in Table 3. The frequencies of the vehicle dynamic corresponding to the four independent DOFs are also presented. The vehicle is assumed moving over the bridge at a speed of 2m/s considering a Class B road surface roughness. The acceleration responses of the vehicle axles are used to extract the CP responses using the proposed signal process framework considering 5% measurement noise. The identified response residuals and the spectra for two vehicle axles are shown

in Figure 19. From the spectra, it can be seen that the vehicle related dynamic component dominates the CP response residual which is quite different with that when light inspection vehicles are used as presented in previous subsections. For vehicle Model 1, the frequency of vehicle bounce $f_{v1,1}$ has higher amplitude than the bridge first frequency. While, for vehicle Model 2, the two obvious peaks in the spectrum are the frequency of vehicle bounce and pitch, $f_{v1,2}$ and $f_{v2,2}$ respectively. The bridge frequencies are not obviously identified. It can be seen that when using the heavy vehicle to excite the bridge, both the bridge and vehicle systems are the actuator and sensor at the same time. The time-varying dynamic modal parameters reveal important non-stationary characteristics regarding to the VBI. However, the extraction of the time-varying dynamic modal parameters from vehicle response is challenging especially when road surface roughness is considered[38]. In this study, the response component related to the first mode of bridge dynamic is extracted using the proposed method from response residual. Hilbert spectrum is used to study the time-frequency properties of the extracted bridge dynamic component. The components and their Hilbert spectra considering two vehicle models are presented in Figure 20. The evolution of the bridge frequency under moving vehicular loads can be clearly observed. The identified time-varying frequency of bridge extracted from the mono-component is compared to the true values from the numerical eigenvalue analysis. In general, the identified trend and amplitude of the instantaneous frequency are similar to the numerical true values except at the two ends. The discordances at the two ends are due to the assumption of static initial conditions of the bridge and the effect of Gibbs phenomenon with the record length of the data. Moreover, the difference of the trend is obvious when different vehicle models are considered.

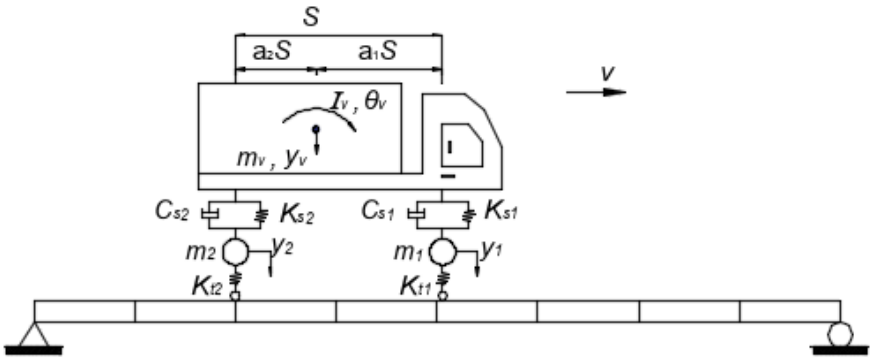

Figure 18 VBI using a two-axle car model

Table 3 Properties of the heavy two-axle car models

Property	Unit	Symbol	Model 1	Model 2
Body mass	kg	m_v	16200	17735
Pitch moment of inertia	kg m^2	Iv	93457	147000

Mass of front axle	kg	m_1	700	1500
Mass of rear axle	kg	m_2	1100	1000
Stiffness of front suspension	N/m	K_{s1}	4.00e5	2.47e6
Stiffness of rear suspension	N/m	K_{s2}	1.00e6	4.23e6
Damping of front suspension	N s/m	C_{s1}	1.00e4	3.00e4
Damping of rear suspension	N s/m	C_{s2}	2.00e4	4.00e4
Stiffness of front tyre	N/m	K_{t1}	1.75e6	3.74e6
Stiffness of rear tyre	N/m	K_{t2}	3.50e6	4.60e6
Axle distance	m	S	4.75	4.27
Axle distance ratio		a_1/a_2	0.50/0.50	0.52/0.48
Frequency of vehicle bounce	Hz	f_{v1}	1.00	2.29
Frequency of vehicle pitch	Hz	f_{v2}	1.55	1.61
Frequency of front axle hop	Hz	f_{v3}	8.83	10.35
Frequency of rear axle hop	Hz	f_{v4}	10.21	15.10

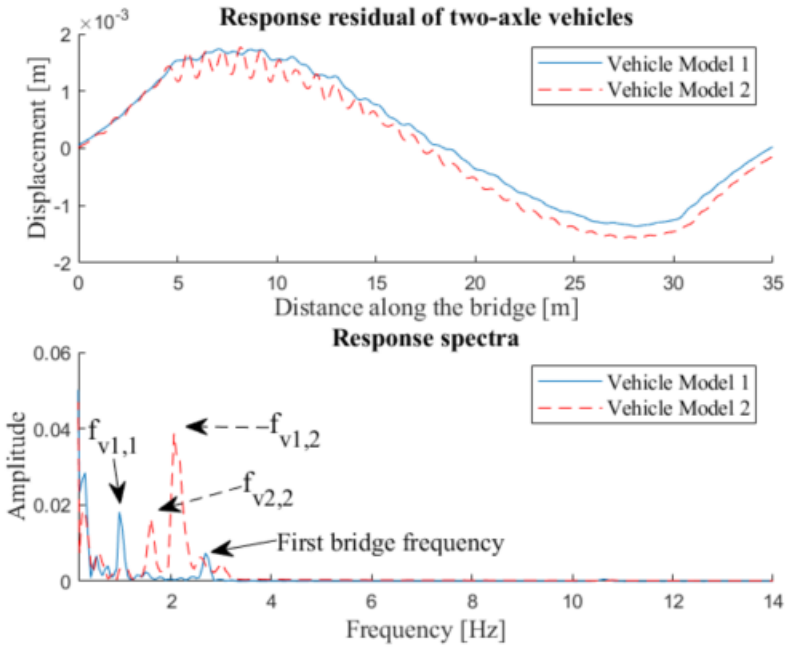

Figure 19 Identified response residuals of two-axle vehicles

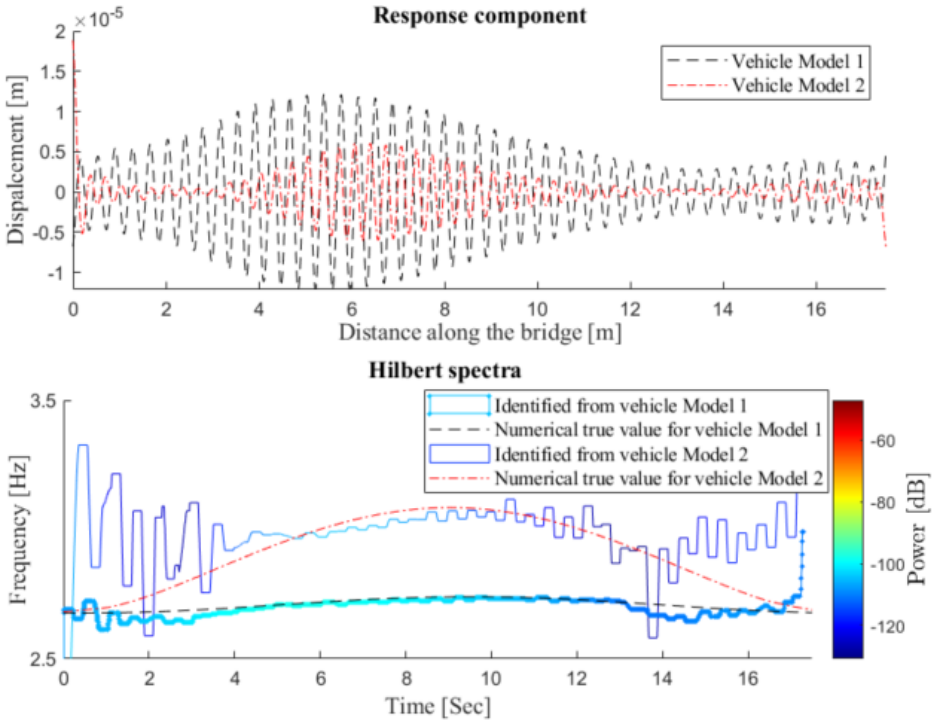

Figure 20 Extracted bridge dynamic components and Hilbert spectra

3.5 Discussions

From above studies, some discussions on the proposed method can be summaries as following: (1). The method can use more sophisticated inspection vehicle models without limiting to SDOF or single-axle vehicles[24-25]. To reduce the effects of road surface by using subtraction technique, no requirement on the using of identical inspection vehicles is needed; (2). Even though the measurement noise has large effects on the identification of CP responses using DKF, the incorporation of Auto SSA to the CP response residual can reduce the effect of noise and extract more bridge dynamic information. However, it is still worthwhile to explore noise-robust joint state-input estimate methods for further improvement of the identification[39]; (3). The proposed method successfully extracts mono-components related to the bridge dynamic response. The bridge modal frequencies are identified from these components in this study. Moreover, it has been theoretically analyzed that the mono-components related to bridge dynamic response extracted from the CP response residual also contain the information of damping ratio under certain assumptions[7]. The identification of damping ratios based on the proposed framework will be further explored in the future; (4). The extracted bridge related mono-component maintains the nonstationary characteristics of VBI when the heavy vehicles are used which can be further processed to reveal the time-varying properties of bridge dynamic under vehicle loads.

4 Experimental study

To verify the proposed method for the extraction of bridge dynamic components via CP response identification based on DKF and Auto SSA, a vehicle-bridge interaction test was conducted on the model built in the laboratory, as shown in Figure 21. The bridge model as shown in Figure 21(a) consists of three rectangular steel beams with width and depth of 100mm and 15mm, respectively. The main beam in the middle is a two equal span continuous simply supported bridge model with a total length of 6m. A leading and trailing beam are placed before and after the main beam to allow for acceleration and deceleration of the vehicle and the length of these beams is 3m. A two-axle vehicle model was fabricated as shown in Figure 21(b). The spacing of the two axles is 0.30 m and the mass of the vehicle is 4.9kg. The wheel of the vehicle model is made of plastic rubber with a light mass and large stiffness. The masses m_1, m_2 for the front and rear axles of the vehicle are very small and ignored. The spring above the wheel to support the vehicle body is considered as the suspension system of the vehicle model. Therefore, when compared to the typical 4-DOF two-axle vehicle model as shown in Figure 16, the experimental vehicle is simplified as a 2-DOF system only considering the vertical displacement and pitching motion of the vehicle body. Modal testing was carried out on the main beam and the first two natural frequencies were obtained as 5.68 and 8.48 Hz, respectively. The first vehicle frequency is 29.36Hz. A wireless sensory system was set up for the test with wireless accelerometer sensors, BeanDevice AX-3D. The sensors were installed on the front and rear axles of the vehicle as shown in Figure 21(b). Laser sensors were installed to record the time instants when the vehicle arrives at and exits from the main beam. The sampling frequency for the measurement was 500 Hz. Plastic strips with different thickness were attached to the surface of the beam to simulate bumps on the road. The model vehicle was pulled along the beam with an electric motor. The detailed description of the tests can be found in [26].

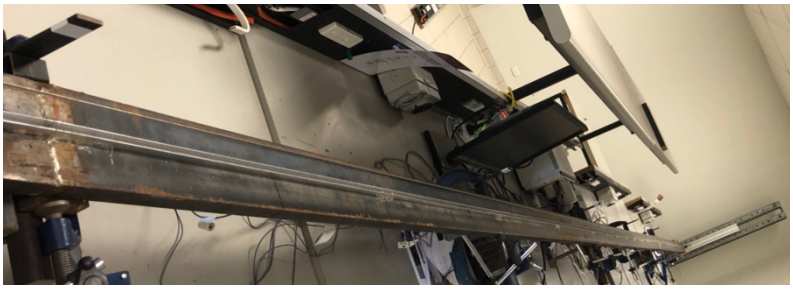

(a) The bridge model

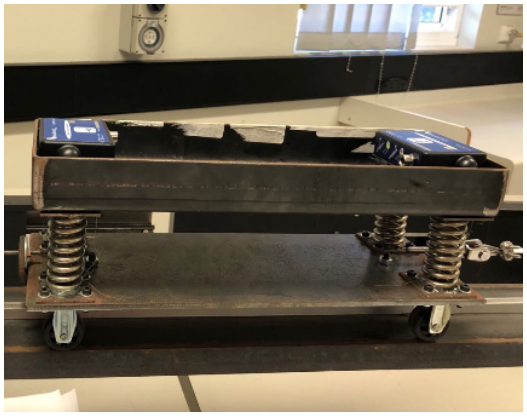

(b) The vehicle model

Figure 21 Vehicle-bridge interaction model in the lab

Figure 22 shows the measured responses of the vehicle when it passed over the main beam with a speed about 0.36m/s. The proposed method is used to identify the contact-point responses from the vehicle responses. The response residual of contact points estimated by using DKF and the response residual of measured vehicle responses along with their spectra are shown in Figure 23. It can be seen that the bridge modal parameters are very difficult to be identified from the residual of vehicle responses due to the dynamic component of vehicle. On the contrary, when the residual of the CP responses is used, the vehicle dynamic component is eliminated so that the bridge related dynamic parameters can be identified more readily. The mono-component related to the bridge dynamic is extracted using Auto SSA and the results are given in Figure 24. The identified bridge modal frequency is very close to the first bridge modal frequency obtained from modal test. The results demonstrate the effectiveness of the proposed method in enhancing the drive-by bridge modal identification by suppressing the vehicle dynamic components.

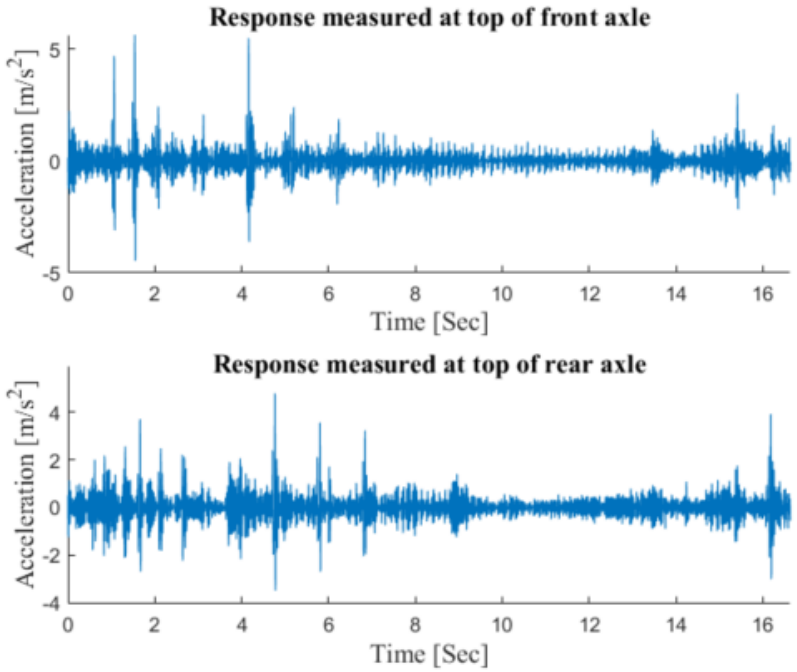

Figure 22 The measurement data of vehicle responses

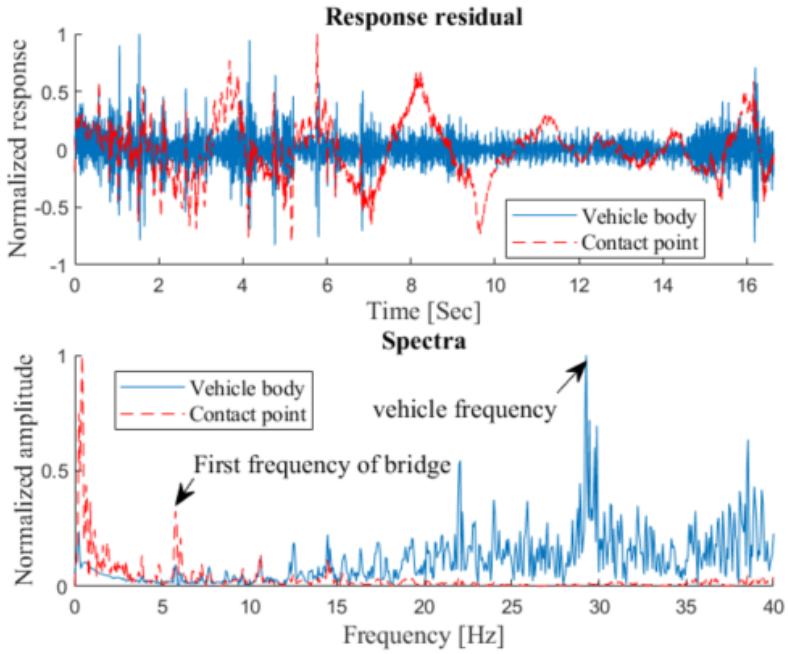

Figure 23 Response residuals of vehicle and contact point and their spectra

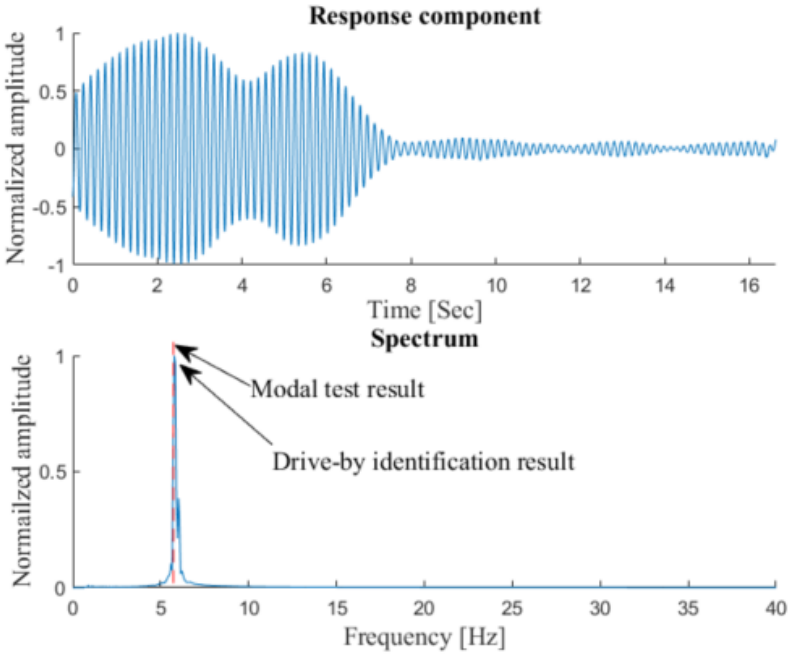

Figure 24 Extraction of bridge related dynamic component

5 Conclusions

The extraction of bridge dynamic components from vehicle responses is challenging when road surface roughness is considered. The vehicle and driving related dynamic component can make the bridge related dynamic component blurred. In this study, a signal process method consisting of three steps is proposed to isolate the bridge dynamic components from noisy vehicle responses. The dual Kalman filter is first applied to obtain the input forces of two successive vehicles accurately using vehicle responses and to identify the CP responses. The response residual of two contact points is then calculated by subtraction of the identified CP responses. The bridge dynamic component is finally extracted from the response residual using Auto SSA for modal identification. The results of numerical and experimental studies demonstrate the effectiveness of the proposed method in enhancing the drive-by bridge modal identification despite the effects of road surface roughness.

Acknowledgements

This research is supported in part by research funding of the National Natural Science Foundation of China (52078461, 52108288, 51878433, U1709207,), the Key R&D program of Zhejiang (2019C03098) and the Postdoctoral Science Foundation of Zhejiang Province (ZJ2020024). The financial aid is gratefully acknowledged.

Appendix A

The explicit Newmark-β method [30] is based on an assumed variation $\ddot{\mathbf{x}}$ of acceleration between two time steps, i.e. $\ddot{\mathbf{x}}_k$ and $\ddot{\mathbf{x}}_{k+1}$, as

$$\ddot{\tilde{\mathbf{x}}} = (1-\gamma)\ddot{\mathbf{x}}_k + \gamma\ddot{\mathbf{x}}_{k+1} \qquad (0 \le \gamma \le 1) \tag{a1}$$

$$\ddot{\tilde{\mathbf{x}}} = (1-2\beta)\ddot{\mathbf{x}}_k + 2\beta\ddot{\mathbf{x}}_{k+1} \qquad (0 \le \beta \le 0.5) \tag{a2}$$

Integrating the acceleration between t_i and t_{i+1}, the displacement $\mathbf{x}_{i+1}$ and velocity $\dot{\mathbf{x}}_{i+1}$ at t_{i+1} can be obtained as

$$\dot{\mathbf{x}}_{k+1} = \dot{\mathbf{x}}_k + \Delta t\ddot{\tilde{\mathbf{x}}} \tag{a3}$$

$$\mathbf{x}_{k+1} = \mathbf{x}_k + \Delta t\dot{\mathbf{x}}_k + \tfrac{1}{2}\Delta t^2\ddot{\tilde{\mathbf{x}}} \tag{a4}$$

The iterative form of the explicit Newmark-β method is obtained as [32]

$$\begin{bmatrix}\mathbf{x}_{k+1}\\ \dot{\mathbf{x}}_{k+1}\\ \ddot{\mathbf{x}}_{k+1}\end{bmatrix} = \begin{bmatrix}\mathbf{A}_0\\ \mathbf{B}_0\\ \mathbf{C}_0\end{bmatrix}\mathbf{D}F_{cp}{}_{k+1} + \begin{bmatrix}\mathbf{A}_d & \mathbf{A}_v & \mathbf{A}_a\\ \mathbf{B}_d & \mathbf{B}_v & \mathbf{B}_a\\ \mathbf{C}_d & \mathbf{C}_v & \mathbf{C}_a\end{bmatrix}\begin{bmatrix}\mathbf{x}_k\\ \dot{\mathbf{x}}_k\\ \ddot{\mathbf{x}}_k\end{bmatrix} \tag{a5}$$

where $\mathbf{A}_0 = (\mathbf{K} + \frac{1}{\beta\Delta t^2}\mathbf{M} + \frac{\gamma}{\beta\Delta t}\mathbf{C})^{-1}$, $\mathbf{A}_d = \mathbf{A}_0(\frac{1}{\beta\Delta t^2}\mathbf{M} + \frac{\gamma}{\beta\Delta t}\mathbf{C})$, $\mathbf{A}_v = \mathbf{A}_0\left[\frac{1}{\beta\Delta t}\mathbf{M} + (\frac{\gamma}{\beta} - 1)\mathbf{C}\right]$, $\mathbf{A}_a = \mathbf{A}_0\left[(\frac{1}{2\beta} - 1)\mathbf{M} + \frac{\Delta t}{2}(\frac{\gamma}{\beta} - 2)\mathbf{C}\right]$, $\mathbf{C}_0 = \frac{1}{\beta\Delta t^2}\mathbf{A}_0$, $\mathbf{C}_d = \frac{-1}{\beta\Delta t^2}\mathbf{A}_0\mathbf{K}$, $\mathbf{C}_v = \frac{-1}{\beta\Delta t^2}\mathbf{A}_0(\mathbf{C} + \Delta t\mathbf{K})$,

$\mathbf{C}_a = \frac{1}{\beta\Delta t^2}\mathbf{A}_0\left[(\gamma - 1)\Delta t\mathbf{C} - \beta\Delta t^2(\frac{1}{2\beta} - 1)\mathbf{K}\right]$, $\mathbf{B}_0 = \frac{\gamma}{\beta\Delta t}\mathbf{A}_0$, $\mathbf{B}_d = \frac{-\gamma}{\beta\Delta t}\mathbf{A}_0\mathbf{K}$,

$\mathbf{B}_v = \frac{\gamma}{\beta\Delta t}\mathbf{A}_0\left[\left(\frac{\beta\Delta t}{\gamma} - \Delta t\right)\mathbf{K} + \frac{1}{\gamma\Delta t}\mathbf{M}\right]$, $\mathbf{B}_a = \frac{-\gamma}{\beta\Delta t}\mathbf{A}_0\left[\left(\frac{\beta\Delta t^2}{\gamma} - \frac{\Delta t^2}{2}\right)\mathbf{K} + (\frac{1}{\gamma} - 1)\mathbf{M}\right]$.

$$\mathbf{A} = \begin{bmatrix}\mathbf{A}_d & \mathbf{A}_v & \mathbf{A}_a\\ \mathbf{B}_d & \mathbf{B}_v & \mathbf{B}_a\\ \mathbf{C}_d & \mathbf{C}_v & \mathbf{C}_a\end{bmatrix}, \qquad \mathbf{B} = \begin{bmatrix}\mathbf{A}_0\\ \mathbf{B}_0\\ \mathbf{C}_0\end{bmatrix}\mathbf{D}.$$

Reference

[1] Yang, Y. B., Lin, C. W., and Yau, J. D. (2004). Extracting bridge frequencies from the dynamic response of a passing vehicle. *Journal of Sound and Vibration*, 272(3): 471-493.

[2] Zhu, X. Q., and Law, S. S. (2015). Structural health monitoring based on vehicle-bridge interaction: accomplishments and challenges. *Advances in Structural Engineering*, 18(12), 1999-2015.

[3] Jian, X. D., Xia, Y., and Sun, L. M. (2020). An indirect method for bridge mode shapes identification based on wavelet analysis. *Structural Control and Health Monitoring*, 27(12), e2630.

[4] Kim, C. W., Isemoto, R., McGetrick, P. J., Kawatani, M., and O'Brien, E. J. (2014). Drive-by bridge inspection from three different approaches. S*mart Structures and Systems*, 13(5), 775-796.

[5] Shi, Z. H., and Uddin, N. (2021). Extracting multiple bridge frequencies from test vehicle – a theoretical study. *Journal of Sound and Vibration*, 490, 115735.

[6] González, A., O'Brien, E. J., and McGetrick P. J. (2012). Identification of damping in a bridge using a moving instrumented vehicle. *Journal of Sound and Vibration,* 331(18): 4115-4131.

[7] Yang, Y. B., Zhang, B., Chen, Y. A., Qian, Y., Wu, Y. T. (2019). Bridge damping identification by vehicle scanning method. *Engineering Structures*, 183: 637-645.
[8] Zhang, Y., Wang, L. Q., and Xiang, Z. H. (2012). Damage detection by mode shape squares extracted from a passing vehicle. *Journal of Sound and Vibration*, 331(2): 291-307.
[9] Li, J. T., Zhu, X. Q., Law, S. S., and Samali, B. (2019). Indirect bridge modal parameters identification with one stationary and one moving sensors and stochastic subspace identification. *Journal of Sound and Vibration*, 446: 1-21.
[10] Hester, D., and González, A. (2017). A discussion on the merits and limitations of using drive-by monitoring to detect localised damage in a bridge. *Mechanical Systems and Signal Processing*, 90, 234-253.
[11] Yang, Y. B., and Chang, K. C. (2009). Extraction of bridge frequencies from the dynamic response of a passing vehicle enhanced by the EMD technique. *Journal of Sound and Vibration*, 322(4–5), 718-739.
[12] Eshkevari, S. S., Matarazzo, T. J., and Pakzad, S. N. (2020). Bridge modal identification using acceleration measurements within moving vehicles. *Mechanical Systems and Signal Processing*, 141, 106733.
[13] Flandrin, P., Rilling, G., and Goncalves, P. (2004). Empirical mode decomposition as a filter bank. *IEEE Signal Processing Letters*, 11(2), 112-114.
[14] Liu, K., Law, S. S., Xia, Y., and Zhu, X. Q. (2014). Singular spectrum analysis for enhancing the sensitivity in structural damage detection. *Journal of Sound and Vibration*, 333(2), 392-417.
[15] Panda, R., Jain, S., Tripathy, R. K., Sharma, R. R., and Pachori, R. B. (2021). Sliding mode singular spectrum analysis for the elimination of cross-terms in wigner–ville distribution. *Circuits, Systems, and Signal Processing*, 40(3), 1207-1232.
[16] Li, J. T., Zhu, X. Q., Law, S.S., and Samali, B. (2019). Drive-by blind modal identification with singular spectrum analysis. *Journal of Aerospace Engineering*, 32(4), 04019050.
[17] Elsner, J. B. and Tsonis, A. A. (1996). Singular spectrum analysis, a new tool in time series analysis. Plenum Press.
[18] McNeill, S., and Zimmerman, D. (2008). A framework for blind modal identification using joint approximate diagonalization. *Mechanical Systems and Signal Processing*, 22(7), 1526-1548.
[19] Yang, Y. B., Li, Y. C., and Chang, K. C. (2012). Using two connected vehicles to measure the frequencies of bridges with rough surface: a theoretical study. *Acta Mechanica*, 223 (8): 1851–1861.
[20] Malekjafarian, A. and O'Brien, E. J. (2014). Identification of bridge mode shapes using short time frequency domain decomposition of the responses measured in a passing vehicle. *Engineering Structures*, 81: 386-397.
[21] O'Brien, E. J., McGetrick, P. J., and Gonzalez, A. (2014). A drive-by inspection system via vehicle moving force identification. *Smart Structures and Systems*, 13(5), 821-848.
[22] Zhu, X. Q., Law, S. S., Huang, L., and Zhu, S. Y. (2018). Damage identification of

supporting structures with a moving sensory system. *Journal of Sound and Vibration*, 415, 111-127.

[23] ElHattab, A., Uddin, N., and O'Brien, E. J. (2017). Drive-by bridge damage detection using non-specialized instrumented vehicle. *Bridge Structures*, 12(3-4), 73-84.

[24] Yang, Y. B., Zhang, B., Qian, Y., and Wu, Y. T. (2018). Contact-point response for modal identification of bridges by a moving test vehicle. *International Journal of Structural Stability and Dynamics*, 18(05), 1850073.

[25] Nayek, R., and Narasimhan, S. (2020). Extraction of contact-point response in indirect bridge health monitoring using an input estimation approach. *Journal of Civil Structural Health Monitoring*, 10(5), 815-831.

[26] Li, J. T., Zhu, X. Q., Law, S. S., and Samali, B. (2020). A two-step drive-by bridge damage detection using dual Kalman filter. *International Journal of Structural Stability and Dynamics*, 20(10), 2042006.

[27] Harmouche, J., Fourer, D., Auger, F., Borgnat, P., and Flandrin, P. (2018). The sliding singular spectrum analysis: a data-driven nonstationary signal decomposition tool. *IEEE Transactions on Signal Processing*, 66(1), 251-263.

[28] Henchi, K., Fafard, M., Talbot, M., and Dhatt, G. (1998). An efficient algorithm for dynamic analysis of bridges under moving vehicles using a coupled modal and physical components approach. *Journal of Sound and Vibration*, 212(4), 663-683.

[29] ISO-8608, *Mechanical Vibration-Road Surface Profiles-Reporting of Measured Data*, International Organization for Standardization (ISO), Geneva (1995).

[30] Liu, K., Law, S. S., Zhu, X. Q., and Xia, Y. (2014). Explicit form of an implicit method for inverse force identification. *Journal of Sound and Vibration*, 333(3), 730-744.

[31] Azam, S. E., Chatzi, E., and Papadimitriou, C. (2015). A dual Kalman filter approach for state estimation via output-only acceleration measurements. *Mechanical Systems and Signal Processing*, 60, 866-886.

[32] Hassani, H. (2007). Singular spectrum analysis: methodology and comparison. *Journal of Data Science*, 5(2), 239-257.

[33] Ward, J. H. (1963). Hierarchical grouping to optimize an objective function. *Journal of the American Statistical Association*, 58(301), 236-244.

[34] Alamdari, M. M., Kildashti, K., Samali, B., and Goudarzi, H. V. (2019). Damage diagnosis in bridge structures using rotation influence line: validation on a cable-stayed bridge. *Engineering Structures*, 185, 1-14.

[35] Sadeghi Eshkevari, S., Matarazzo, T. J., and Pakzad, S. N. (2020). Simplified vehicle–bridge interaction for medium to long-span bridges subject to random traffic load. *Journal of Civil Structural Health Monitoring*, 10(4), 693-707.

[36] Cebon, D. (1999). *Handbook of vehicle-road interaction.* Swets and Zeitlinger, Lisse, Netherlands.

[37] Law, S. S., and Zhu, X. Q. (2004). Dynamic behavior of damaged concrete bridge structures under moving vehicular loads. *Engineering Structures*, 26(9), 1279-1293.

[38] Li, J. T., Zhu, X. Q., Law, S. S., and Samali, B. (2020). Time-varying characteristics of bridges under the passage of vehicles using synchroextracting

transform. *Mechanical Systems and Signal Processing*, 140, 106727.

[39] Lei, Y., Lu, J. B., and Huang, J. S. (2020). Synthesize identification and control for smart structures with time-varying parameters under unknown earthquake excitation. *Structural Control and Health Monitoring*, 27(4), e2512.